

In presenting the dissertation as a partial fulfillment of the requirements for an advanced degree from the Georgia Institute of Technology, I agree that the Library of the Institute shall make it available for inspection and circulation in accordance with its regulations governing materials of this type. I agree that permission to copy from, or to publish from, this dissertation may be granted by the professor under whose direction it was written, or, in his absence, by the Dean of the Graduate Division when such copying or publication is solely for scholarly purposes and does not involve potential financial gain. It is understood that any copying from, or publication of, this dissertation which involves potential financial gain will not be allowed without written permission.

7/25/68

ORDER STRENGTHENING IN NICKEL- 20 ATOMIC
PERCENT MOLYBDENUM ALLOY

A THESIS

Presented to
The Faculty of the Graduate Division
by
Bhaven Chakravarti

In Partial Fulfillment
of the Requirements for the Degree
Master of Science in Metallurgy

Georgia Institute of Technology

June 1970

ORDER STRENGTHENING IN NICKEL- 20 ATOMIC
PERCENT MOLYBDENUM ALLOY

Approved:

Chairman

Date Approved by Chairman: 5/26/70

ACKNOWLEDGEMENTS

The author is deeply indebted to his thesis advisor, Dr. Edgar A. Starke Jr., for suggesting this research and his constant encouragement and guidance throughout the project.

A very special thanks is extended to Dr. Bruce G. LeFevre for his tremendous interest in the work and the continued guidance given the author. Without his help in field ion microscopy much would have remained undone.

It gives the author great pleasure to thank Dr. Stephen Spooner for having taken time off from his many and pressing duties to review this work. His interest and criticism is greatly appreciated.

Finally the assistance given by Dr. R. J. Gerdes of The Engineering Experiment Station, for taking the scanning electron micrographs and Mr. Richard Mitchell for preparing the photographs is gratefully acknowledged.

TABLE OF CONTENTS

	Page
ACKNOWLEDGMENTS	iii
LIST OF TABLES	v
LIST OF FIGURES	vi
SUMMARY	viii
Chapter	
I. INTRODUCTION	1
II. LITERATURE SURVEY	4
Phase Relationships	
Structural Studies	
Mechanical Properties	
III. EXPERIMENTAL METHODS	8
Preparation of Specimens	
Examination of Specimens	
IV. RESULTS	12
Tensile Test Results	
Electron Microscopy Results	
Field ion Microscopy Results	
V. DISCUSSION OF RESULTS	27
VI. CONCLUSIONS	33
APPENDIX	34
BIBLIOGRAPHY	40

LIST OF TABLES

Table	Page
1. Compositions of the Alloys Examined	8
2. Results of Tensile Tests After Various Ageing Times With Corresponding Degree of Order and Antiphase Domain Size	13

LIST OF FIGURES

Figure	Page
1. Microhardness of Ni_4Mo at 25°C measured as a function of ageing time at various temperatures after quenching from 1000°C	9
2(a). Scanning Electron Micrograph of Fracture Surface of Ni_4Mo in Disordered Condition	14
2(b). Scanning Electron Micrograph of Fracture Surface of Ni_4Mo in the Ordered Condition	14
3(a). Transmission Electron Micrograph of Ni_4Mo after 40 minutes at 700°C showing fine cross-textured contrast within the grains	16
3(b). Diffraction Pattern from the cross-textured region showing superlattice spots from differently oriented domains	16
4(a). The Heterogeneous Component appearing in the α -grain boundaries after 180 minutes at 700°C	18
4(b). Enlarged View of the Heterogeneous Component	18
5(a). Delta Fringe Contrast from Perpendicular Twins in the Heterogeneous Region	19
5(b). Dark Field Image with a Superlattice Reflection showing Antiphase Boundaries within the Heterogeneous Region	19
6(a). Field Ion Micrograph of Ni_4Mo in Disordered Condition	21
6(b). Field Ion Micrograph of Ni_4Mo Annealed 40 minutes at 700°C	21
6(c). Field Ion Micrograph of Ni_4Mo Annealed 15 Hours at 700°C	21
6(d). Field Ion Micrograph of Ni_4Mo Annealed 300 Hours at 750°C for comparison	21

LIST OF FIGURES (continued)

Figure		Page
7.	Field Ion Micrograph of Ni_4Mo annealed 40 minutes at 700°C taken during Field Evaporation	23
8.	Field Ion Micrograph of Ni_4Mo showing High Density of Perpendicular Twins	25

SUMMARY

The structural modifications which accompany ordering of Ni_4Mo during isothermal ageing at 700°C have been correlated with the mechanical behavior of this material. The ordering reaction was found to proceed homogeneously until late in the process when a heterogeneous reaction was initiated along the grain boundaries. The increase in strength was attributed to the domain size hardening and the stresses induced due to the ordered phase. The decrease in ductility was attributed to either the development of dislocations in coplanar arrays or concentrated slip in the heterogeneous component.

CHAPTER I

INTRODUCTION

It is well known that the deformation behavior of crystals is highly structure sensitive, being influenced by a variety of defects which may be present before, or formed during, the deformation process. If a crystal contains more than one atomic species, a further influence on the mechanical behavior is exhibited by local atomic arrangements. Four general types of arrangements are possible on a particular lattice in a solid solution; (a) random, in which there is no preference by an atom for a type of neighbor or particular lattice site (1,2), (b) short-range ordered, in which a given atomic species exhibits a statistical preference for unlike neighbors but not for a particular lattice site (1,3), (c) clustered, in which a given atomic species exhibit a statistical preference for like neighbors but not for a particular lattice site (4), and (d) long-range ordered, in which the different atomic species occupies preferred sites on the crystal lattice (5,6). The references cited for each arrangement refer to reviews of theories on strengthening mechanisms attributed to these various arrangements.

The present research is concerned with order-strengthening induced when a previously disordered alloy undergoes a transition to long-range order. The transition from random or short-range order to long-range order is initiated at some critical temperature during cooling. The completeness of the transition or the degree of long-

range order may be varied by certain thermal and/or mechanical treatments and is usually described by the LRO parameter S . Warren (7) has defined this parameter as

$$S = (r_A - X_A)/Y_B = (r_B - X_B)/Y_A$$

where r_A and r_B are respectively the fractions of A-sites and of B-sites occupied by the correct atoms, X_A and X_B the atomic fractions of A and B atoms, and Y_A and Y_B the fraction of A and B lattice sites. For a stoichiometric alloy S is, therefore, zero when the alloy is perfectly random and one when perfectly ordered.

Depending on the particular alloy system the ordering may occur either homogeneously or heterogeneously (8). In addition, the crystal system may or may not be altered. Cu_3Au , for example, has a cubic structure both in the ordered and disordered states. In contrast, Ni_4Mo changes from cubic in the disordered condition (α -phase) to tetragonal in the ordered state (β -phase) having a contraction of 0.5% in a_0 and 1.0% in c_0 of the cubic lattice (9).

Alloys which undergo a distortion or crystal structure change during the transition offer the greatest potential in order strengthening. However, there have been only a few studies on alloys of this type, mainly on CuAu (10,11,12). Ni-Mo alloys have been found to respond readily to age-hardening treatments in the β region after quenching from above the transformation temperature (13,14,15). Although the agreement of the data is not particularly good, the investigators all agree that large hardness increases can be produced within a few tenths

of an hour by annealing in the temperature range of 600-800°C. The time-temperature-transformation curve for the ordering process of Ni_4Mo has a "C" shape with the nose of the curve around 710-775°C(16,17). The kinetics and morphology of the ordering process in this alloy has recently received attention (16-23).

The present study was undertaken in an effort to understand order-hardening in alloys which undergo a crystal structure change during ordering. Ni_4Mo was chosen for study since previous experience showed this alloy to be conducive to microscopic studies by x-ray diffraction, electron and field-ion microscopy techniques. It was felt that structural modifications which accompany the disorder-order transitions and which could be correlated with mechanical property measurements would help elucidate order-strengthening in Ni_4Mo alloy.

CHAPTER II

LITERATURE SURVEY

Phase Relationship

Most of the earlier literature of the nickel-molybdenum system dealt with the determination of the constitutional diagram. This problem has since been resolved and an extensive review on this phase of the research can be found in references (24,25). The Ni_4Mo alloy has a face-centered cubic (FCC) structure above 868°C and transforms by a peritectoid reaction (Appendix A) to an ordered body-centered tetragonal (BCT) unit cell, which is two and half times larger than the FCC unit cell. The α to β transformation can result in thirty possible orientations, though only six will produce unique orientation-relationships between the α and β phases (13).

Since the α to β transformation proceeds isothermally it is assumed to occur by a diffusion process. No evidence has yet been presented that would indicate a shear type transformation, nor the occurrence of a metastable phase (64). The orientation relationship of the α to β phase suggests that the transformation should occur with the β phase existing in a coherent or partially coherent state. However, due to the tetragonal lattice contraction upon ordering and the high degree of strain that accompanies it, there will be a tendency for the zones to lose coherency with the matrix. The β phase may consequently prefer to nucleate at imperfections such as dislocations where much of the accompanying strains

of transformation can be accommodated (10).

Structural Studies

Spruiell (18) studied the short-range order (SRO) in the nickel-molybdenum system by x-ray diffuse scattering measurements on single crystals containing 10.7 and 20.0 atomic percent molybdenum. He found SRO in both alloys where quenched from above their critical temperatures. Further annealing at lower temperature increased the diffuse intensity maxima showing an increase in SRO. On annealing the 20.0 at % molybdenum alloy at 650°C he found the diffuse intensity maxima present immediately after quenching to split into doublets and sharpen considerably. The diffuse intensity appeared to gradually approach the sharp intensity distribution of the fully ordered Ni_4Mo structure. He concluded that SRO in nickel-molybdenum alloys was similar to the Ni_4Mo type of long-range order. Thus the transition to LRO from SRO would be continuous and just a matter of domain size, the SRO structure being but the "microdomains" of the LRO structure. McManus (26) found the SRO measured on polycrystalline samples of Ni_4Mo agreed with Spruiell's (18) conclusion on the absence of molybdenum-molybdenum nearest neighbors.

Baer (27) studied the SRO in single crystals of Ni_4W , which shows the same type of diffuse scattering as Ni_4Mo , and concluded that the domain structure of Ni_4Mo LRO was not the proper model for SRO in Ni-W. He suggested a model in which alternate double layers of (420) planes were nickel rich and nickel poor compared to the random solution. The enrichment and depletion was about 4 percent. Antiphase boundaries should be able to form in such a model, though it is improbable that this slight

departure from randomness could be responsible for the observed domain boundaries.

Ruedl et al. (19), observed 10\AA "microdomains" in electron micrographs of quenched alloy, and suggested that ordering occurred through microdomain growth. However, Clapp and Moss (28) suggest that the statistical model of SRO was probably more correct.

Ruedl et al. (19) classified the substructure resulting from ordering into three classes; (a) translation antiphase boundaries, as observed in other ordered alloys, (b) antiparallel twins, where the c-axis of adjacent domains were antiparallel, (c) perpendicular twins, where the c-axis of the adjacent domains were perpendicular. In the last case either the c-axis was coupled head to head (or tail to tail) or head to tail (or tail to head). Only in the case of head to tail coupling would the two structures be mirror images or twins. Various examples of these domain boundaries have been shown (19). LeFevre and Newman (22) showed that with the field ion microscope the domain boundaries are easily characterized and the direction of rotation of the ordered unit cell can be determined.

Mechanical Properties

Ruedl et al. (19) theoretically envisioned various glide paths on the $(111)_C$ planes in the Ni_4Mo structure and showed that they could be 4, 6, or 10 fold glide superdislocations. Such total dislocations were made up of a number of partial dislocations and antiphase boundaries; for example a 4 fold glide path is a superdislocation split into partials with antiphase boundary in between. No such superdislocations were

observed by them in their electron microscopic study. Brooks et al. (29) studying the dislocation structure in nickel-molybdenum alloys, found that cross-slip was restricted. They concluded that the stacking fault energy decreased on ordering. Such restriction of cross-slip could also be due to the SRO present in the quenched alloy.

Snyder and Brooks (23) have recently studied the mechanical properties of Ni_4Mo . The yield strength of the alloy approximately doubled within five minutes of ageing at 775°C . Concurrent with it, the alloy virtually lost its ductility. On further ageing the yield strength decreased continuously and after ten hours it was less than the as quenched value, however, the alloy remained brittle. The maximum yield strength of the alloy was at some intermediate degree of order. They explain this behavior using Stoloff and Davies's theory (5) which correlates the strength maximum with the point where the superdislocation spacing (which depends on the degree of order) become so large, that they dissociate into unit dislocations.

CHAPTER III

EXPERIMENTAL METHODS

Preparation of Specimens

Alloys were prepared by arc-melting in argon atmosphere from high purity nickel and molybdenum to form Ni_4Mo . Each sample was melted six times to insure adequate mixing of the nickel and molybdenum. The as-cast ingots were cold rolled to a 50 percent reduction in thickness to break up the cast structure, homogenized in vacuum at 1000°C for one week and quenched in iced brine. They were then rolled to a thickness of 0.38 cm. and machined to a thickness of 0.32 cm.

The composition of the samples were determined from lattice parameter measurements made on stress-relieved-325 mesh fillings using high purity aluminum as an internal standard. The data of Guthrie and Stansbury (13) were used for calculating the composition from the lattice parameter measurements. The compositions of the samples used in this study are given in Table I.

Table I. Composition of the Alloys Examined

<u>Alloy No.</u>	<u>Weight%</u>	<u>Atomic%</u>	<u>Alloy No.</u>	<u>Weight%</u>	<u>Atomic%</u>
A0	27.30	18.69	D180	27.80	19.07
B40	27.85	19.10	E154	27.40	18.76
C100	27.55	18.88			

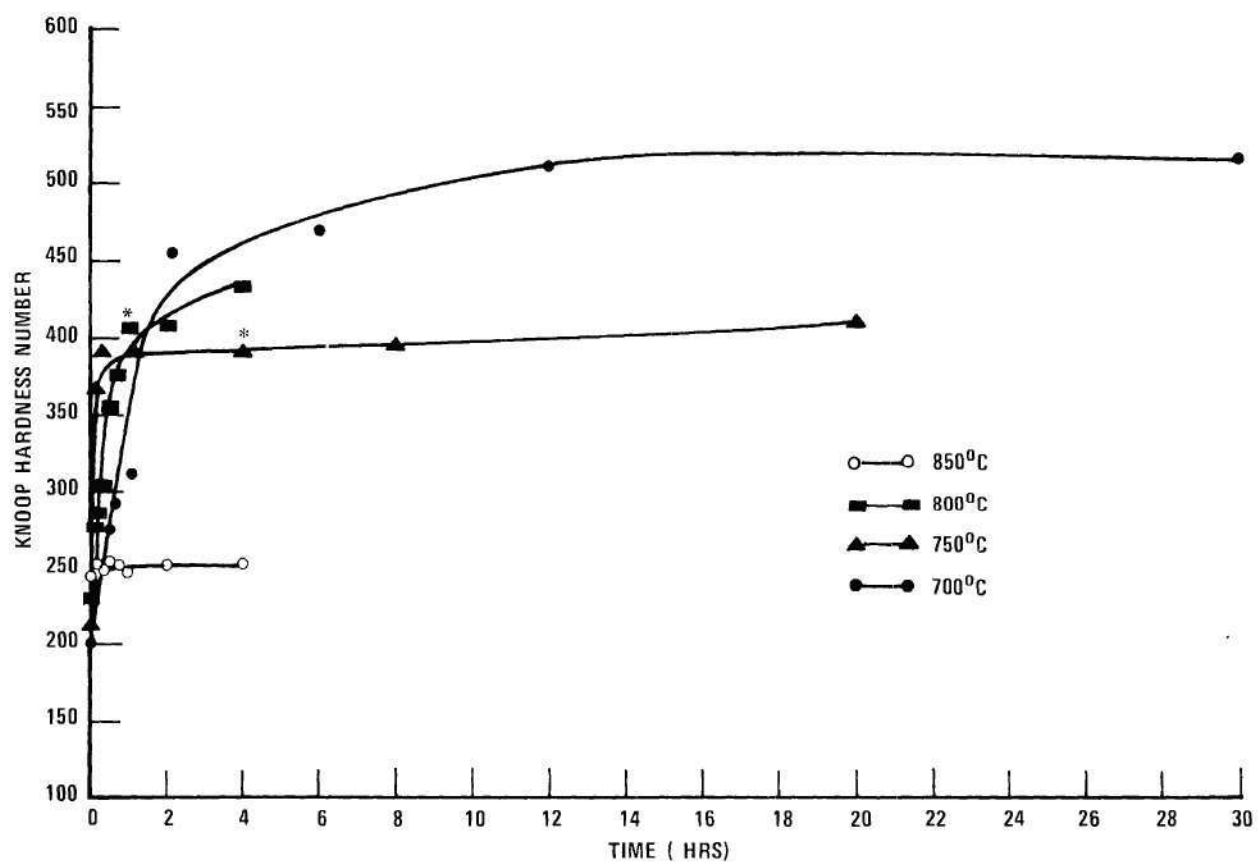


Figure 1. Microhardness of Ni_4Mo at 25°C Measured as a Function of Ageing Time at Various Temperatures After Quenching from 1000°C .

Tensile samples were machined according to ASTM-66 for subsize specimens. The stresses induced by the machining operation were removed during a final disordering heat treatment of 5 hours at 1000°C followed by iced brine quenching.

The ordering temperature and times to be used for extensive study were determined by preliminary investigations using hardness measurements. Samples 1 cm. square were ordered in vacuum for various times at 700, 750, 800 and 850°C. The hardness was measured using a Tukon Tester and a 500 gram load. The critical ordering temperature has been given as 868°C (13). The results of these measurements are given in Figure 1. There was no response to the 850°C heat treatment even after four hours, so treatments at this temperature were discontinued. The hardening rate at both 750 and 800°C were adequate, however the ordering process induced cracks in the samples. The times and the temperatures at which cracking was observed are denoted by asterisks in Figure 1. No cracking was ever observed on samples treated at 700°C although a marked increase in hardness was observed after short times at this temperature. Consequently, 700°C was chosen for the ordering treatments for structural-mechanical property correlations.

Examination of Specimens

The degree of order after various heat treatments was determined by x-ray techniques using monochromated $\text{CuK}\alpha$ radiation and a modified GE XRD-6 diffractometer described elsewhere (30). The preferred orientation of the samples combined with the supposition of the fundamental and superlattice reflections of polycrystalline Ni_4Mo necessitated the usage of

the technique devised by LeFevre and Starke (31) for order parameter determination. The order parameter was measured on each tensile sample prior to testing. The average domain size was also determined by x-ray diffraction using Scherrer's equation. The $(110)_T^*$ superlattice peak was used for these calculations and was corrected for strain and instrumental broadening by comparison with the nearby $(211)_T$ fundamental peak.

The tensile tests were conducted on an Instron testing machine using a one-inch extensometer and a strain rate of 0.05 per minute. Three samples (A0, C100, E15H) were pulled to fracture and two others to about 5 percent plastic strain. The fracture surfaces were examined by scanning electron microscopy using a Cambridge Stereoscan Mark II. Slices were spark cut from each of the tensile samples, ground to 0.025 cm. and small discs punched out for observation in the electron microscope. The discs were jet polished at 0°C using a solution of two parts sulphuric acid and one part water. Electron microscopic observations were made in transmission in both a Siemens 1A and JEM 7A microscopes at 100KV. Samples for field-ion studies were cut from similar slices used for electron microscopy. The field-ion samples were electro-polished in the sulphuric acid solution to fine wire form and imaged in Helium at liquid hydrogen temperature.

* Sub T refers to the tetragonal indices and sub C refers to the cubic indices.

CHAPTER IV

RESULTS

The ordering sequence of Ni_4Mo has been followed at 700°C by structural and mechanical studies. Tensile tests provided strength and fracture data of the alloy at various stages of the ageing process. X-ray diffraction techniques were employed along with electron and field-ion microscopy to obtain detailed information on the nature of the structure responsible for the mechanical properties, and to elucidate the ordering mechanism.

Tensile Test Results

Table 2 gives the results of the tensile tests after various ageing times along with the corresponding degree of order and antiphase domain size as determined from x-ray measurements. The yield stress rises sharply initially but levels off after an ageing treatment of 100 minutes. The total increases in strength of $4,100 \text{ kg/cm}^2$ and work hardening coefficient of 18.3×10^2 after 15 hours ageing were accompanied by a change in the LRO parameter from zero to one and an increase in the antiphase domain size to 106 \AA . In addition the elongation decreased from 60% in the disordered sample to 3.2% in the fully ordered sample and was accompanied by a change in fracture mode from transgranular, Figure 2a, to intergranular, Figure 2b.

Table 2. Results of tensile tests after various ageing times with corresponding degree of order and antiphase domain size.

Alloy Number	Ageing Time	Degree of Order 'S'	Domain Size in Å	Yield Stress in kg/cm ²	Percent Elongation	Percent Red. in Area	Work Hardening Coefficient x 10 ²
A0	Quenched	0.0	-	3,500	60.0	43.0	33.7
B40	40 min.	0.64	46	6,200	-	-	-
C100	100 min.	0.76	54	6,720	26.0	22.4	36.8
D180	180 min.	0.81	74	7,340	-	-	-
E15H	15 hrs.	1.00	106	7,635	3.2	3.15	52

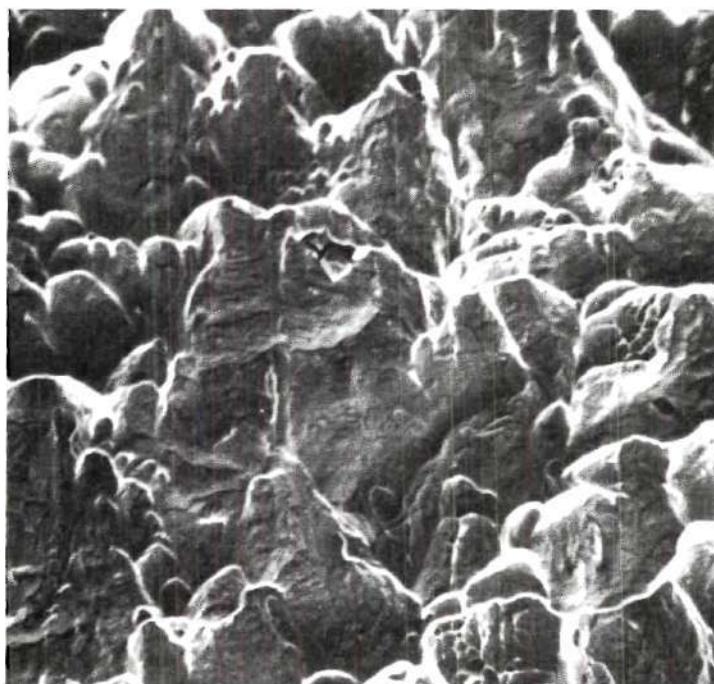


Figure 2a. Scanning Electron Micrograph of Fracture Surface of Disordered Ni_4Mo . (1970x)

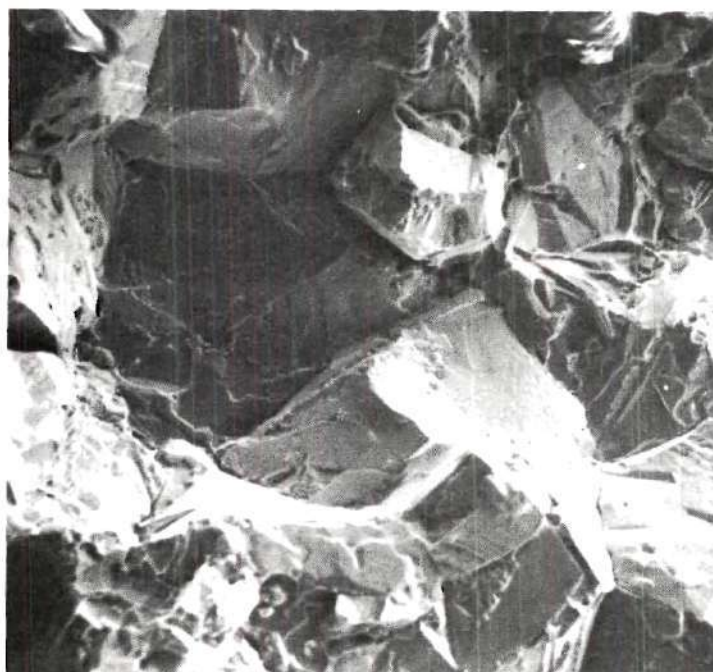


Figure 2b. Scanning Electron Micrograph of Fracture Surface of Ordered Ni_4Mo . (580x)

Electron Microscopy Results

The electron microscopy studies showed that the disordered alloy exhibited large equiaxed grains, approximately 40 microns, and numerous annealing twins indicating a completely recrystallized structure. Considerable short-range order was present, as evidenced by the appearance of diffuse spots in the electron diffraction pattern (18,19,23), and numerous paired dislocations in the micrographs (32-36). A very fine "mottle" contrast was visible in the vicinity of the bend extinction contours similar to that observed by Ruedl et al. (19) and Snyder and Brooks (23). Dark field images obtained by placing the objective aperture over a diffuse spot failed to show any distinct microdomains in the short-range-ordered structure.

The ordering transformation of Ni_4Mo at 700°C was revealed by the electron microscopy studies to occur by two distinct mechanisms. The early stage was characterized by the development of a fine cross-textured contrast appearing uniformly within the grains. A representation of this stage, which will be referred to as the "homogeneous component" is presented in Figure 3a which characterizes a sample aged for 40 minutes at 700°C . The contrast was produced by an operating fundamental reflection and the striations were shown by standard trace analysis methods to be approximately parallel to $\{112\}_\text{C}$ plane traces. Selected area diffraction patterns showed the presence of superlattice spots from all of the six possible domain orientations. However, the usual antiphase boundary contrast present in ordered alloys (37) was never observed even with extensive tilting of the specimen. This was assumed to be due to

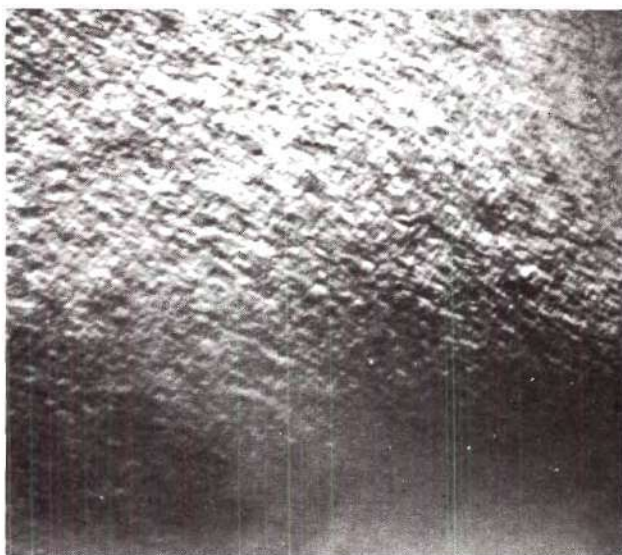


Figure 3a. Transmission Electron Micrograph of Ni₄Mo After 40 Minutes at 700°C Showing Fine Cross-Textured Contrast within the Grains. (40,000x)

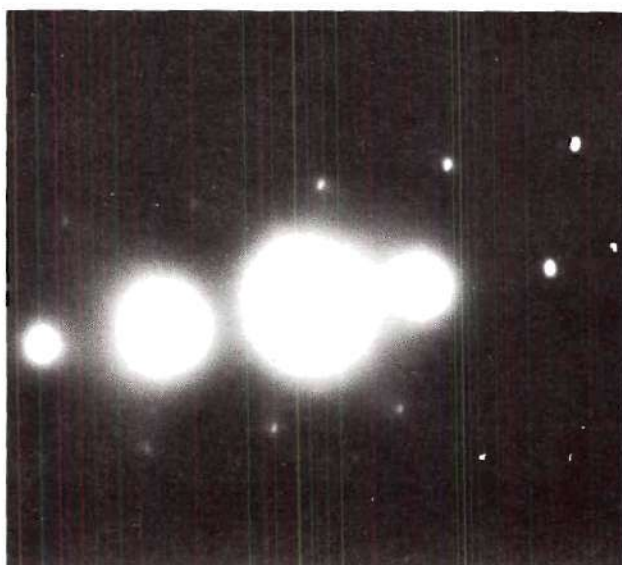


Figure 3b. Diffraction Pattern from the Cross-Textured Region Showing Superlattice Spots from Differently Oriented Domains.

the fineness of the structure which was verified by field-ion microscopy to be discussed later. No distinct rellods were observed in the diffraction patterns as one might expect from small particle or strain effects (Figure 3b). Further annealing at 700°C for a total time of 100 minutes produced no significant changes in either the micrographs or the electron diffraction patterns except for a slight coarsening of the cross-textured contrast.

After 180 minutes a second ordering mechanism was initiated as shown by the presence of a "heterogeneous component" which appeared at the α -grain boundaries, Figure 4. Such contrast effects have been observed in Ni_4Mo after ageing at 775°C (23) as well as in other ordering systems involving a cubic to tetragonal transition (10,23,38). The contrast within the heterogeneous region is very similar to the appearance of the columnar grain structure in a metal casting with the long dimension perpendicular to the grain boundary. Close inspection, Figure 4b, shows that along one edge it appears to be continuous with the homogeneous component of one grain while along the opposite edge it is separated from the continuous component of the adjacent grain by a sharp and apparently incoherent interface. Tanner (39) has described a similar reaction product in Ni_2V as a coherent allotriomorph which forms coherently with one grain and grows into the adjacent grain by migration of the incoherent grain boundary. A similar effect in CuAu has been described by Arunachalam and Cahn (10) as recrystallization by stress induced boundary migration.

The heterogeneous component grew continuously with further ageing and after 15 hours at 700°C it comprised approximately one-third of the

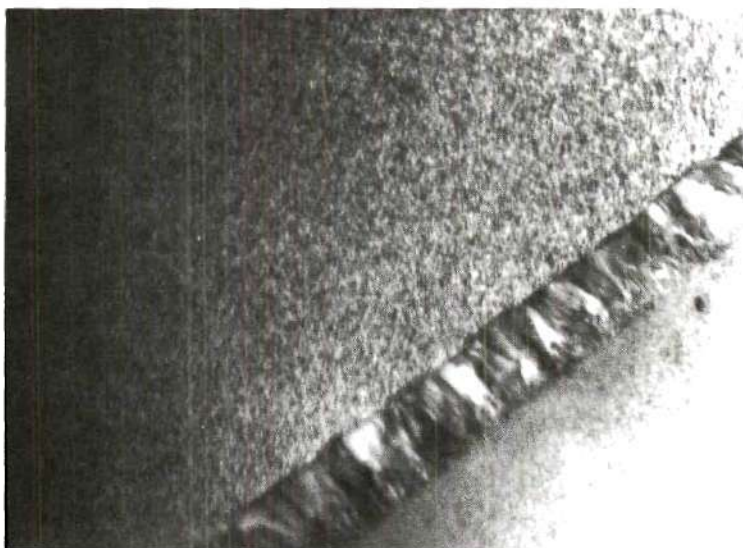


Figure 4a. The Heterogeneous Component Appearing in the α -Grain Boundaries After 180 Minutes at 700°C. (20,000x)



Figure 4b. Enlarged View of the Heterogeneous Component. It is Continuous with the Homogeneous Component Along a-a' but Discontinuous Along b-b'. (40,000x)



Figure 5a. δ -Fringe Contrast from Perpendicular Twins in the Heterogeneous Region. (20,000x)



Figure 5b. Dark Field Image with a Superlattice Reflection Showing Antiphase Boundaries within Heterogeneous Region. (50,000x)

total volume of the structure. Contrast effects from the various type of interfaces (antiparallel twin boundaries, perpendicular twin boundaries and antiphase boundaries) previously discussed by Ruedl et al. (19) were clearly distinguishable in this region (Figure 5a and 5b). The perpendicular twins indicated by the δ -fringes of Figure 5a were found to be very thin platelets lying parallel to $\{110\}_C$ planes. By careful tilting of the foil it was determined that in most cases what appeared to be the boundary between adjacent twin related domains was, in fact, an entire twinned region so thin its boundaries completely overlapped. This was further supported by field-ion microscopy studies.

Field-ion Microscopy Results

The field-ion studies were undertaken to elucidate more precisely the nature of the microstructure of the alloy in the partially ordered state. From the available x-ray and electron microscopy data one cannot accurately determine the domain size and shape nor how the degree of order varies locally within a microstructure such as that exhibited in Figure 3a. For the purpose of this study it was important to know whether the fine cross-textured contrast was indicative of a structure which was truly homogeneous or heterogeneous, i.e., a two-phase mixture of ordered and disordered regions. The difficulty of differentiating contrast effects due to phase boundaries from those due to coherency strains in electron micrographs of a fine structure such as this has been stressed by Tanner (38,40). On the other hand it has been shown that field-ion images can be used to determine the domain structure and obtain a qualitative measure of the order parameter on an atomic scale (21,22,41-46).

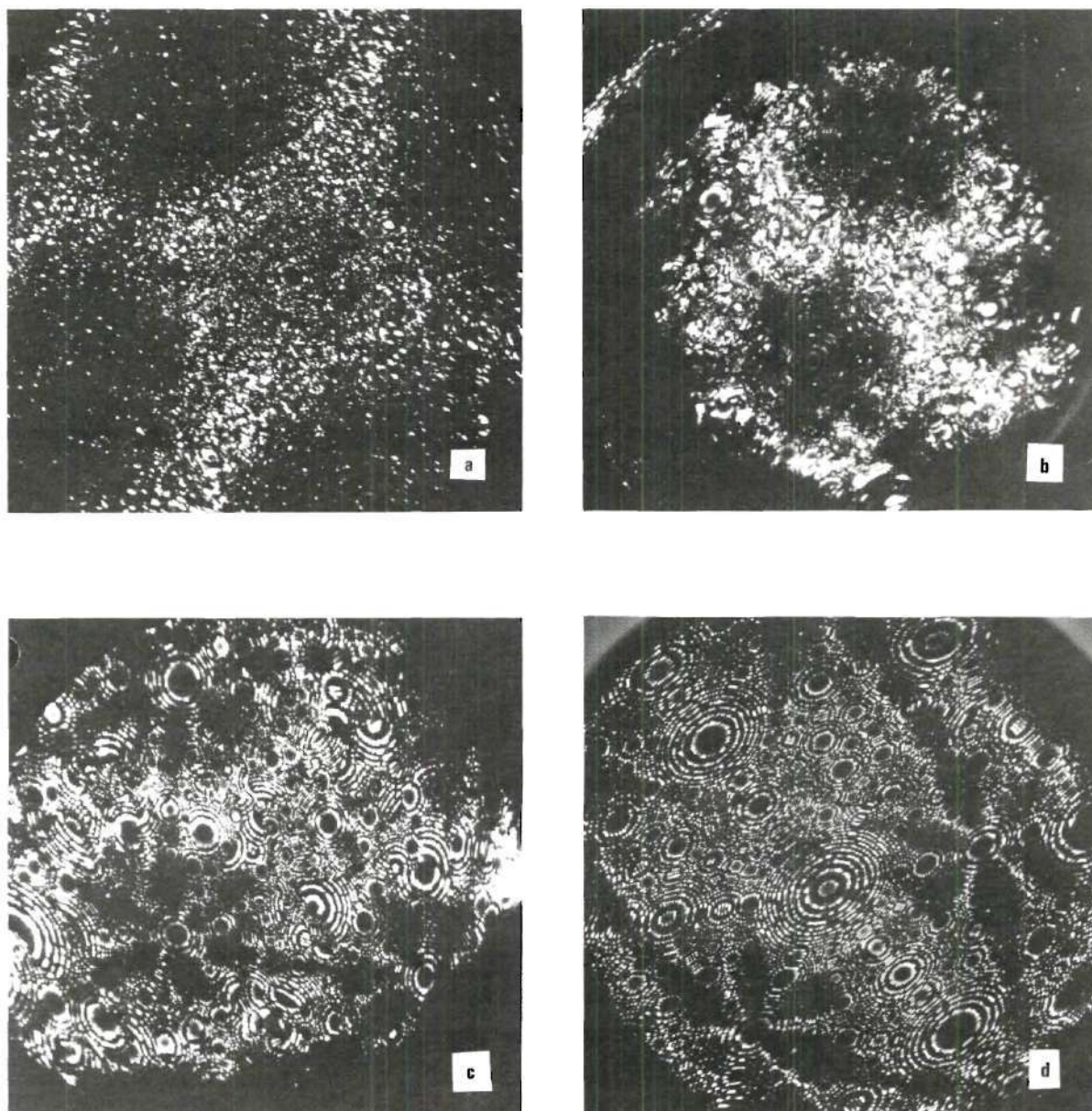


Figure 6. Field Ion Micrographs of Ni_4Mo in Various Conditions: (a) Disordered; (b) Annealed 40 Minutes at 700°C ; (c) Annealed 15 Hours at 700°C ; (d) Annealed 300 Hours at 750°C to Produce Fully-Ordered Large Domains for Comparison.

Field-ion micrographs depicting the microstructure of the homogeneous component are presented in Figure 6. The treatment of the sample represented by Figure 6d was not a direct part of the present study and serves only as an aid in interpretation. The degree of order is represented in the microstructure by the local regularity of the image and the domain boundaries by discontinuities in the image symmetry (21). It can be seen that the 40 minute anneal produced a microstructure of uniformly ordered material consisting of many contiguous domains in which the order is less than perfect. No evidence was ever seen in such images of the coexistence of ordered and disordered regions^{*} as one would expect in a classic nucleation and growth process. Hence this structure has the appearance one would expect from a homogeneous ordering process. The fact that the image is somewhat less regular than that of the fully ordered structure of Figure 6d is in qualitative agreement with the LRO parameter of 0.6 determined by x-ray measurements. This was further reflected by the lack of complete stability of the specimen during the imaging process. It is characteristic of this material that disordered specimens are in a dynamic state of irregular field evaporation during imaging whereas the completely ordered specimens are quite stable.

^{*}The regional darkness seen in these micrographs is not to be confused with heterogeneity in the structure. This occurs in the vicinity of low index poles of the cubic lattice and results from the effect of crystallographic anisotropy on the basic imaging process

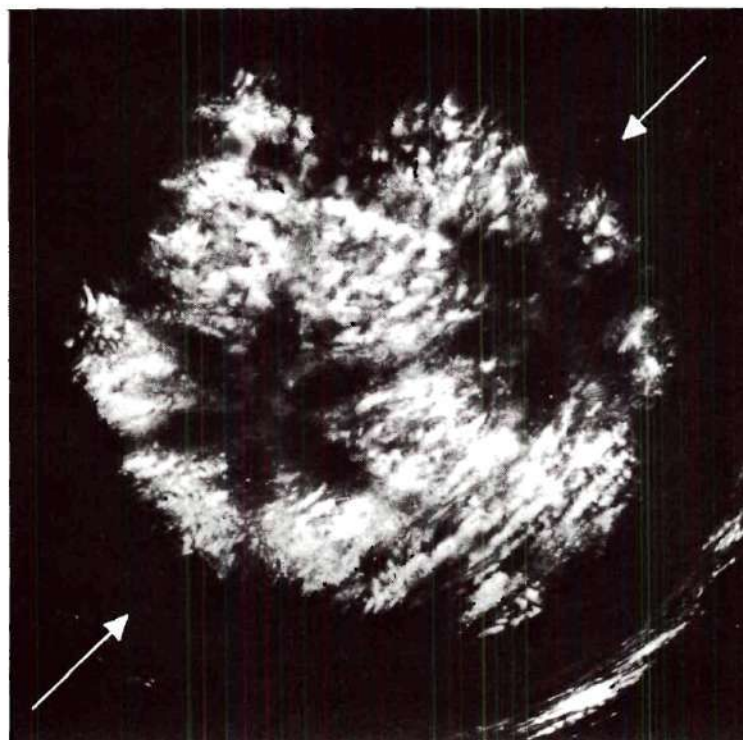


Figure 7. Field Ion Micrograph of Ni_4Mo Annealed 40 Minutes at 700°C and Taken During Field Evaporation. The Domains Show a Tendency to be Elongated in a Direction Parallel to the Arrows.

The average domain size of the 40 minutes anneal appears to be in the range of 20 to 50 \AA^{**} which is also in rough agreement with the domain size determined from the x-ray measurements. It is clear from this evidence why individual domains were not resolved in the electron microscope. The domain network can be made to show more prominently by photographing the specimen during field evaporation, as shown in Figure 7. It can be seen that the domains show a tendency to be elongated in a direction indicated by the arrows. Within the accuracy of this analysis this direction was found to be parallel to a $\{112\}_C$ plane trace in agreement with the orientation of the striations in the electron micrographs. This observation is significant because there appears to be some question as to whether similar striae in other systems represent the true domain shape or simply the direction of attendant coherency strains. It would appear that in Ni_4Mo one is seeing the true domain shape in the fine striae of the electron micrographs. The changes in the structure of the homogeneous component with increasing ageing times can be seen by comparing Figure 6b with Figure 6c. The domains increase in size from the 20 to 50 \AA° present after 40 minutes to 100 to 200 \AA° after 15 hours, and the degree of order within the domains also increases. The results are in agreement with the electron microscopy and x-ray results.

Figure 8 shows a specimen with an extremely high density of the thin plate-like perpendicular twins photographed during field evaporation

* Field-ion micrographs approximate pseudo-sterographic projections. Since the linear magnification varies from center to edge, micron markers would not be meaningful; however, a rough measure of the magnification can be obtained from the fact that the linear distance across the imaged region of each of the micrographs is approximately 1500-2000 \AA° .

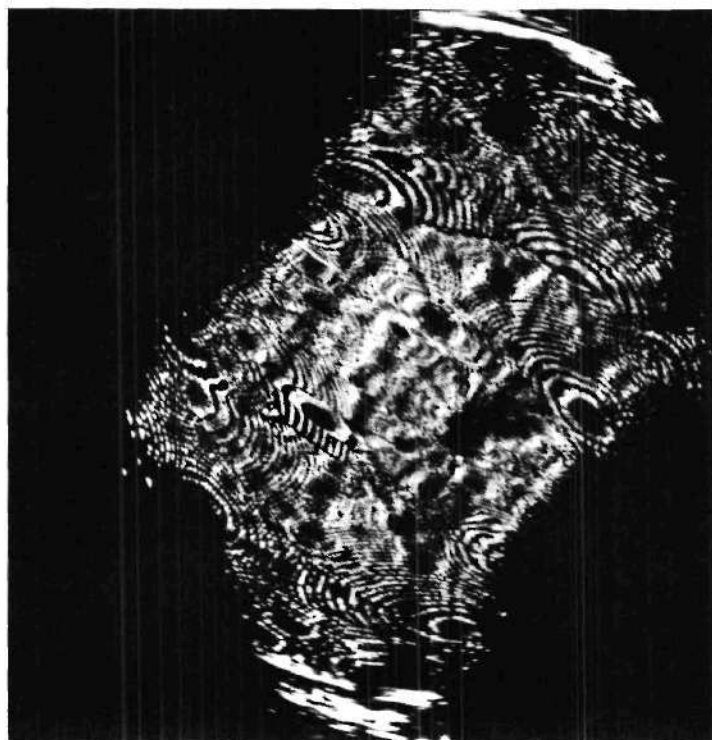


Figure 8. Field Ion Micrograph of Ni_4Mo Showing High Density of Perpendicular Twins. Annealed at 750°C for 20 Hours.

to enhance the appearance of the boundaries. The anneal given (750°C for 20 hours) was again not a direct part of the present study; however, it was known from prior experience that such a condition produces a high density of the twins so that the maximum probability of encountering them in the field-ion specimen would exist. It can be seen here that many of the twins are only a few atomic diameters thick as was concluded in the electron microscopy results discussed earlier.

CHAPTER V

DISCUSSION OF RESULTS

Ordering of Ni_4Mo

The usual controversy which surrounds most discussions on order-disorder reactions; i.e., whether or not they should be considered as first or second order transformations, will not be discussed here. It should not be necessary to prove that in a system such as Ni_4Mo , in which the ordered and disordered states differ in crystal structure, that the ordering reaction could be anything but a classical phase change; i.e., a first order transformation (47). Instead, the present discussion will concentrate on the mechanism by which the Ni_4Mo alloy proceeds from the disordered to the ordered state. Transformations cannot be classified as to first or second order on the basis of kinetic considerations since these can be greatly varied by seemingly insignificant changes in heat-treatment procedure.

The ordering of Ni_4Mo below the critical temperature T_c , has been considered to proceed by nucleation and growth of microdomains which exist above T_c . This concept was first presented by Spruiell (18) who suggested a model for short-range order above T_c similar to long-range ordered Ni_4Mo . Experimental support for this model has been presented by Ruedl et al. (19). In addition, Synder and Brooks (23) have used this concept in discussing isothermal ordering of Ni_4Mo at 775°C . On the other hand, theoretical considerations of interaction energies have led Clapp and Moss (28) to

suggest that the microdomain theory might not be particularly useful in this system and that the short-range order could best be explained by the statistical theory.

There have been many discussions on other systems which undergo a crystal structure change during ordering as to whether the reaction occurs homogeneously or by nucleation and growth (48-53). The presence of microdomains above T_c has suggested to some workers (54) a nucleation and growth concept below T_c , whereas the statistical SRO model might imply homogeneous ordering below this temperature. The concept of microdomains above the critical temperature has actually been very hazily defined. These domains are normally considered to be of small size and vary in degree of order. As the size of the domains decreases the statistical model for short-range order is approached and the domains lose their individual identity (55). Likewise concepts of homogeneous ordering and a nucleation and growth process in Ni_4Mo during isothermal ordering below T_c merge as the annealing temperature is reduced. The volume free energy of ordering increases with decreasing temperature and for Ni_4Mo the interface coherency strain energy also decreases with decreasing temperature. The latter result may be inferred from dilatometry measurements of Stansbury (56). The variation of these parameters with temperature indicate that as the aging temperature is lowered small nuclei become more stable and the frequency of nucleation is increased (53). Consequently, at a "low aging temperature" the frequency of nucleation is so high and the nuclei so small that the material is homogeneous kinetically, impingement between the domains is instantaneous and there is essentially no "two

phase" region between an ordered nucleus or microdomain and a disordered matrix. After impingement the mobility of the boundaries is reduced since there is no change in composition or structure across the interface. Ordering then proceeds by atomic rearrangement within the domains of the stoichiometric alloy.

This model is supported by the field-ion microscopy of the present study. No domains of ordered structure were observed in the disordered matrix of samples quenched from above the critical temperature. In addition, no "two phase" structure was observed at any stages of partial order at 700°C. Instead, the ordered regions always impinged, and appeared homogeneous. The order within the domains after short ageing times was imperfect and corresponded closely with that measured by x-ray diffraction techniques. It is interesting to note that the size of the domains in the early stages of ordering, i.e., closely approximates the size of the microdomains calculated by Spruiell (18) for short-range order above T_c .

In the late stages of homogeneous ordering a heterogeneous reaction was initiated at the prior α grain boundaries. This structure, which appeared to be coherent with one grain and incoherent with the adjacent one, Figure 4, consumed the small domains by the motion of the incoherent interface. The driving force for this process was most likely the decrease in energy of the system obtained by eliminating the antiphase boundaries between the small domains. This heterogeneous component has previously (10,23) been attributed to a spontaneous recrystallization process which eliminates the ordering stresses. While this is certainly possible it is felt that the present explanation is more feasible for

Ni_4Mo for the following reasons: (a) the process does not occur to any extent at high temperatures (23) (b) ordering in Ni_4Mo at low temperatures should produce less concentrated stresses than high temperature ordering since the domains are smaller, and the lattice parameters of the ordered and disordered phases differ to a lesser degree (56). The infrequent occurrence of the heterogeneous reaction at 775°C can then be attributed to the formation of large nuclei and a low nucleation frequency resulting in a large domain size (23).

Although the present study did not include "high temperature" investigations, the ideas presented above on ordering in Ni_4Mo are not inconsistent with the results of other workers at higher temperatures (23).

Mechanical Behavior

The remarkable mechanical property changes which accompany ordering reactions have been attributed to a variety of mechanisms (3,5,6). Since many of these mechanisms can operate simultaneously in an alloy, it is very difficult to present a quantitative discussion of their effects. Therefore, only a qualitative correlation between the structure and the mechanical behavior of Ni_4Mo will be attempted.

Any discussion of the mechanical properties of ordered alloys must be made in terms of dislocation motion. It has been shown (5,6) that one significant factor is whether slip dislocations move singularly or in pairs as superdislocations. In view of the small domain structure observed at all stages of ageing in the present study, this factor will be considered first. The diameter of these domains was less than the calculated value

of the spacing between paired dislocations of most ordering systems (5). Similar calculations were made for Ni_4Mo by assuming the glide plane to be $\{111\}_C$ and the superdislocation to be composed of pairs of unit dislocations of the type $1/2 \langle 110 \rangle_C$. The antiphase domain boundary energy for these calculations was determined using a modification of Flinn's (57) method (see appendix B). The separation was determined for various degrees of order for the most favorable condition for splitting, i.e., for a pure edge total dislocation. In all cases, except for $S \leq 0.2$, the separation was less than the corresponding domain size indicating a high probability for the presence of superdislocations in this system.

The improvement in strength of Ni_4Mo during ordering at 700°C can be attributed to both the domain size and the degree of order. Cottrell (58) has suggested a strengthening mechanism which depends on the creation of new domain boundary as slip dislocations intersect old boundaries. This mechanism should contribute significantly in the present case since the domains are relatively small. However, since their size is approximately constant after 40 minutes of ageing this mechanism does not account for the continuous rise in strength. This must be explained in terms of the development of the ordered structure within the domains. It cannot, however, be attributed to the destruction of order by dislocation motion since the motion of superdislocations does not destroy order across the glide plane. However the ordering process in Ni_4Mo produces a tetragonal distortion which resist dislocation motion. Since the distortion increases as the degree of order increases, this effect qualitatively explains the continuous strength increase during ageing.

The decrease in ductility with ordering at 700°C can be attributed to a number of factors. One factor is a lowering of the probability of dynamic recovery by cross slip. Another factor is the increased tendency for the formation of coplanar dislocation arrays. This can result from the confinement of dislocations to their slip planes in ordered alloys and the reduction of possible slip systems (59). Once the coplanar arrays are formed, pileups occur at interfaces, such as grain boundaries, and result in large local stresses across the boundaries. When these stresses are sufficient, intergranular fracture occurs. Another mechanism resulting in brittle intergranular fracture may involve the heterogeneous reaction which occurs along the grain boundaries. The antiphase domains in these regions are large compared to the fine domain structure of the homogeneous component. These regions should be softer owing to the presence of fewer domain boundaries and the higher probability of superdislocation motion. Slip concentrated in these areas could result in failure along the grain boundaries where they are formed.

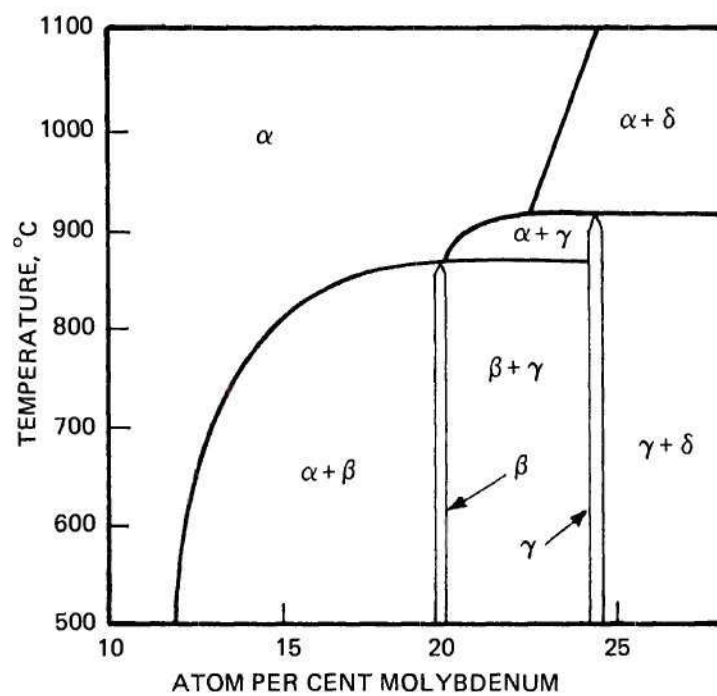
Failure along the grain boundaries during ordering, as was observed in the present study at 750 and 800°C, has been observed in other systems (10), and attributed to the ordering stresses. At 750°C and 800°C the distortions due to the difference in volume of the ordered and disordered phases in Ni_4Mo can cause large internal stresses. The resultant direction and magnitude of these is dependent on the frequency of nucleation and the critical nuclei size.

CHAPTER VI

CONCLUSIONS

1. Ordering of Ni_4Mo at 700°C occurs by a two stage process; initially by the formation of a homogeneous component and finally by the movement of an incoherent interface from the α -grain boundaries to produce the heterogeneous reaction component.
2. In the case of Ni_4Mo the fine striations observed in the electron micrographs represents the true domain size and shape.
3. The tremendous improvement in yield strength during ordering of Ni_4Mo can be attributed to the domain size and more importantly to the continuous increase of tetragonal distortion and the accompanying strains.
4. The drastic reduction of ductility in the alloy on ordering could be due to (a) the formation of coplanar arrays of dislocations on the reduced number of slip planes and/or (b) slip concentrated in the heterogeneous component.

APPENDIX A



The Nickel-Rich Portion of the Ni-Mo System
(After Guthrie and Stansbury (13)).

APPENDIX B

Calculation of Antiphase Boundary Energy

The antiphase boundary energy was calculated using the procedure outlined by Flinn (57) with certain modifications to account for the structure of Ni_4Mo . The basic equation is:

$$\frac{\text{Energy}}{\text{area}} = \left(\frac{\text{atoms}}{\text{area}} \right) \times \left(\frac{\text{wrong bonds}}{\text{atom}} \right) \times \left(\frac{\text{energy}}{\text{wrong bond}} \right) \quad [1]$$

In order to simplify the calculation, the following assumptions were made: (a) only nearest neighbor interactions are significant. (b) The tetragonal contractions accompanying ordering can be neglected. (c) Since Ni-Ni nearest neighbors are present in the ordered structure and Mo-Mo nearest neighbors are absent, the only wrong bonds that need be considered are Mo-Mo nearest neighbors.

The energy per wrong bond according to the Bragg-Williams approximation (60) for an AB alloy is given by

$$v = \frac{kT_c}{2F_A F_B Z} \quad [2]$$

where T_c is the critical ordering temperature, F_A and F_B are the atomic fractions of the components and Z is the coordination number. The parameter v defined by the relation:

$$v = v_{AB} - (v_{AA} + v_{BB})/2 \quad [3]$$

and is based on the fact that for an AB alloy the interchange of an A and B pair results in the conversion of a certain number of correct bonds into equal numbers of wrong A-A and B-B bonds. The coordination number enters the equation by considering the fact that each α site is surrounded by Z β sites. In the present case the situation is somewhat different since each Mo atom is surrounded by 12 Ni sites and each Ni site is surrounded on the average by three Mo and nine Ni sites. When this factor is considered along with the fact that the composition is 1/5 Mo and 4/5 Ni we obtain a weighted average value for \bar{v} according to the equation:

$$\bar{v} = 1/5 \left\{ \frac{kT_c}{2(4/5)(1/5)12} \right\} + 4/5 \left\{ \frac{kT_c}{2(4/5)(1/5)3} \right\} \quad [4]$$

Using a value of 1141°K for T_c we obtain

$$\bar{v} = \frac{\text{Energy}}{\text{wrong bond}} \simeq 14 \times 10^{-14} \text{ ergs}$$

The number of wrong bonds per atom is determined from the expression

$$\sum_{\vec{n}} \vec{t} \cdot \vec{R}_{\vec{n} \text{ hkl}} \quad [5]$$

where \vec{t} denotes a wrong bond vector and \vec{R} is the reciprocal lattice vector of the hkl plane on which the antiphase boundary lies, i.e., $|\vec{R}_{\text{hkl}}| = 1/d_{\text{hkl}}$. The sum is evaluated with the restriction that only positive integral values are considered since this is the necessary condition for the bond to cross the plane. In order to determine the possible wrong bond vectors

\vec{t} , we must first consider the number of unique antiphase translation vectors. Ruedl et al. (19) have shown that for Ni_4Mo there are only two: $\vec{P}_1 = a'_0/5 [210]$ and $\vec{P}_2 = a'_0/5 [130]$ both expressed in tetragonal indices. Because of the symmetry of the crystal structure of Ni_4Mo it is sufficient to calculate the antiphase boundary energy for only one of these vectors, say $\vec{P}_1 = a_0/2 [110]$.

A translation of this type generates three Mo-Mo wrong bonds per Mo atom described by the vectors $\vec{t}_1 = a_0/2 [110]$, $\vec{t}_2 = a_0/2 [0\bar{1}\bar{1}]$, $\vec{t}_3 = a_0/2 [0\bar{1}\bar{1}]$, again expressed in cubic indices.

The number of atoms per unit area in an fcc lattice is given by:

$$d_{hkl}/\text{vol. primitive cell} = 4/a_0^2 \sqrt{h^2 + k^2 + l^2} \quad [6]$$

Since in the present case wrong bonds originate only on Mo atoms, the atomic packing and the stacking sequence of the various hkl planes must be considered. Two types of planes are encountered in this structure (21,61). There are mixed species planes containing both Mo and Ni atoms which give rise only to fundamental reflections and there are single species or layered planes (one layer in five being a Mo layer) which give rise to superlattice as well as fundamental reflections. For the mixed planes a factor of 1/5 must be included in the atoms per area expression given by [6] and for the layered planes the value of $\vec{t}_n \cdot \vec{R}_{hkl}$ must be replaced by unity for values less than five since for this case there can not be more than one wrong bond per atom.

Following the procedure outlined above the antiphase boundary energy was determined for various hkl planes assuming perfect order. The plane of least energy was found to be $\{011\}_C$ and that of maximum energy

to be $\{310\}_C$. These values, along with that of the $\{111\}_C$ are: $E_{011} = 0.28\bar{\nu}/a_o^2$; $E_{310} = 1.27\bar{\nu}/a_o^2$; $E_{111} = 0.37\bar{\nu}/a_o^2$.

Superlattice Dislocation Separation

Ruedl et al. (19) have shown that the possible superdislocation arrangement in Ni_4Mo consists of a pair of $1/2 \langle 110 \rangle_C$ unit dislocation moving on a $\{111\}_C$ glide plane. If the separation of the unit dislocations into partials is neglected the equilibrium spacing between them is determined by a balance between their mutually repulsive force and the attractive force arising from the antiphase boundary energy. This balance leads to the expression (62);

$$r = \frac{Gb^2}{2\pi E_{111} S^2} \left[\frac{\cos(\theta + \pi/3) \cos \theta}{1 - \nu} + \sin(\theta + \pi/e) \sin \theta \right] \quad [7]$$

where r is the separation distance and θ and $\theta + \pi/3$ represent the angles subtended between the Burgers vector and the dislocation line. The term S^2 must be introduced to account for the fact that the antiphase boundary energy is decreased by this factor when $S < 1$ (63). The maximum separation occurs when the total Burgers vector of the superdislocation is in an edge orientation, i.e., $\theta = 150^\circ$. Using relation [7] along with a value of $G = 0.75 \times 10^{-5}$ dyne/ \AA and $\nu = 1/3$ leads to the results below:

<u>Long-range Order Parameter, S</u>	<u>Separation in Å</u>
1.0	5
0.8	8
0.6	14
0.4	31
0.2	125

BIBLIOGRAPHY

1. P.A. Flinn, "Strengthening Mechanisms in Solids," (ASM Seminar, Metals Park, Ohio, 1962).
2. N.R. Fiore and C.L. Bauer, "Progress in Materials Science," editor Bruce Chalmers, 13, No. 2, (Pergamon Press, New York, 1967).
3. J.B. Cohen, "A Brief Review of the Properties of Ordered Alloys," J. of Materials Science, 4 (1969) 1012.
4. A. Kelly and R.B. Nicholson, "Progress in Materials Science," editor Bruce Chalmers, 10, (Pergamon Press, New York, 1963).
5. N.S. Stoloff and R.G. Davies, "Progress in Materials Science," editor Bruce Chalmers, 13, No. 1, (Pergamon Press, New York, 1966).
6. R.W. Cahn, "Local Atomic Arrangements Studied by X-Ray Diffraction," edited by J.B. Cohen and J. Hilliard, (Gordon and Breach, 1967).
7. B.E. Warren, "X-Ray Diffraction," (Addison-Wesley Publishing Company, Reading, Mass., 1969).
8. J.B. Cohen, "Recent Developments Concerning the Order-Disorder Transformation," Paper presented at the 1968 ASM Seminar on Phase Transformations, Detroit, Michigan, October, 1968.
9. D. Harker, Journal of Chemical Physics, 12 (1944) 315.
10. V.S. Arunachalam and R.W. Cahn, Journal of Material Science, 2 (1967) 160.
11. V.I. Syutkina and E.S. Yabovleva, Physica Status Solidi 21 (1967) 465.
12. D.W. Pashley, J.L. Robertson and M.J. Stowell, Philosophical Magazine, 19 (1969) 83.
13. P.V. Guthrie and E.E. Stansbury, "X-Ray and Metallographic Study of the Nickel-Rich Alloys of the Nickel-Molybdenum System II," USAEC Report ORNL-3078, Oak Ridge National Lab., Tennessee, July, 1961.
14. F.H. Ellinger, Trans ASM, 30 (1942), 607.
15. A.N. Dubrovina and Ya.S. Umanskiy, Russian Metallurgy, 4 (1966) 56.

16. S.J. Bloch, "Hardness Changes During the Ordering Reaction of Three Nickel-Molybdenum Alloys," M.S. Thesis, Univ. of Tenn. (1960).
17. B.T. Lampe, "An Investigation of the Order-Disorder Transformation in the Ni-Mo Alloy by Electrical Resistivity Measurements," M.S. Thesis, Univ. of Tenn. (1963).
18. J.E. Spruiell and E.E. Stansbury, Journal of Physics and Chemistry of Solids, 26 (1965) 811.
19. E. Ruedl, P. Delavignette and S. Amelingkx, Phys. Stat. Sol., 28 (1968) 305.
20. B.G. Lefevre, A.G. Guy and R.W. Gould, Trans. Met. Soc. AIME, 242 (1968) 788.
21. B.G. Lefevre, H. Grenga and B. Ralph, Phil. Mag., 18 (1968) 1127.
22. B.G. Lefevre and R.W. Newman, "The Study of Ordered Alloys by Field Ion Microscopy " Proceedings of Symposium on Field-Ion Microscopy in Physical Metallurgy and Corrosion, Georgia Institute of Technology, Atlanta, Ga., May 1968.
23. W.B. Snyder and C.R. Brooks, "Mechanical Properties and Domain Structure of Ordered Ni₄Mo," presented at the Third Bolton Landing Conference, Sept. 1969. (to be published).
24. J.E. Spruiell in "X-Ray Study of Short Range Order in Nickel Alloys Containing 10.7 and 20.0 Atomic Percent Molybdenum," PhD Thesis, Univ. of Tenn., 1963.
25. B.G. Lefevre, "Ordering and K-State in Nickel-Molybdenum Alloys", Univ. of Florida, 1966.
26. G.M. McManus, Journal of Applied Physics, 36 (1965) 3631.
27. H.G. Baer, Zeitschrift Fur Metallkunde, 57 (1966) 318.
28. S.C. Moss and P.C. Clapp, "Correlation Functions of Disordered Binary Alloys - III," Technical Report No. 156, Ledgemont Laboratory, Lexington, Mass., Nov. 1967.
29. C.R. Brooks, J.E. Spruiell and C.K.H. Dubose, Materials Research Bulletin, 3 (1968) 381.
30. E.A. Starke, Jr. and E.U. Lee, Mat'l. Res. Bull., 2 (1967) 231.
31. B.G. Lefevre and E.A. Starke, Jr., "Advances in X-Ray Analysis," Vol. 12 (plenum Press, New York, 1969) p. 113.

32. P.R. Swann and J. Nutting, Journal of Institute of Metals, 90, (1961) 133.
33. G. Thomas, Acta Metallurgica, 11 (1963) 1369.
34. W. Bell, W.R. Roser and G. Thomas, Acta Met. 12 (1964) 1247.
35. W. Bell, P. Okamoto and G. Thomas, Acta Met. 13 (1965) 559.
36. Y. Calvayrac and M. Fagard, Comptes Rendus de L'Academie Des Sciences, 258, (1964) 4531.
37. M.J. Marcinkowski, "Electron Microscopy and Strength of Crystals," (John Wiley, New York, 1963), p. 333.
38. L.E. Tanner, Phys. Stat. Sol. 30 (1968) 685.
39. L.E. Tanner, "The Transformation to Long-Range Order in Ni_2V ," presented at the Third Bolton Landing Conference, Sept. 1969 (to be published).
40. L.E. Tanner, Phil. Mag. 14 (1966) 111.
41. H.N. Southworth and B. Ralph, Phil. Mag. 14 (1966) 383.
42. R.W. Newman and J.J. Hren, Phil. Mag. 16 (1967) 211.
43. T.T. Tsong and E.W. Muller, J. Appl. Phys. 38 (1967) 545.
44. T.T. Tsong and E.W. Muller, J. Appl. Phys. 38 (1967) 3531.
45. T.T. Tsong, Surface Science 10 (1968) 303.
46. B. Ralph, "Field-Ion Microscopy", editors J.J. Hren and S. Ranganathan (Plenum Press, New York, 1968).
47. F.N. Rhines and J.B. Newkirk, Trans. ASM 45 (1953) 1029.
48. G. Borelis, J. Inst. Metals 74 (1948) 17.
49. G.C. Kuczynski, R.F. Hockman and M. Doyama, J. Appl. Phys. 26 (1955) 871.
50. J.L. O'Brien and G.C. Kuczynski, Acta Met. 7 (1959) 803.
51. J.B. Newkirk, A.H. Geisler, D.L. Martin and R. Smoluchowski, Trans. AIME 188 (1950) 1249.
52. T.T. Tsong and E.W. Muller, J. Appl. Phys. 38 (1967) 545.

53. H.N. Southworth and B. Ralph, "Conference on Mechanisms of Phase Transformations in Crystalline Solids," (Manchester, July 1968, Institute of Metals).
54. P.S. Rudman, "Intermetallic Compounds," editor J.H. Westbrook, (John Wiley and Sons, New York, 1967).
55. J.W. Cristian, "The Theory of Transformations in Metals and Alloys," (Pergamon Press, Oxford, 1965) p. 202.
56. E.E. Stansbury and J.R. Riddle, private communication.
57. P.A. Flinn, Trans. AIME 218 (1960) 145.
58. A.H. Cottrell, "Properties and Microstructure," (ASM, Cleveland, Ohio, 1954).
59. N.S. Stoloff and R.G. Daview, Acta Met. 12 (1964) 473.
60. W.L. Bragg and E.J. Williams, Proceedings of Royal Society A145 (1934) 699; A 151 (1935) 54; E.J. Williams, Proc. Roy. Soc. A 152 (1935) 231.
61. B.G. Lefevre, E.A. Starke, Jr., and S. Spocner, Surf. Sci. 14 (1969) 266.
62. J. Friedel, "Dislocations," (Addison-Wesley Publishing Co., Reading, Mass., 1964).
63. M.J. Marcinkowski and D.S. Miller, Phil. Mag. 6 (1961) 871.
64. T. Saburi, K. Komatso and S. Nenno, Phil. Mag. 20 (1969) 1091.